

Supporting Information

Theoretical study on the molecular stacking interactions and charge transport properties of triazasumanene crystals-from explanation to prediction

Xi Chen,^a Hidehiro Sakurai,^b Huan Wang,^a Simeng Gao,^a Hong-Da Bi,^c and Fu-Quan Bai,^{*d,e}

^a College of Chemistry and Chemical Engineering, Northeast Petroleum University, Daqing, 163318, China.

^b Division of Applied Chemistry, Graduate School of Engineering, Osaka University, Osaka, 565-0871, Japan.

^c State Grid Heilongjiang Electric Power Company Limited, China.

^d Laboratory of Theoretical and Computational Chemistry, Institute of Theoretical Chemistry and College of Chemistry, Jilin University, Changchun, 130023, China. E-mail: baifq@jlu.edu.cn

^e Beijing National Laboratory for Molecular Sciences, China.

Comparison of Sum and TAS molecules: the N-doping effect on the geometries and electronic structures of sumanene

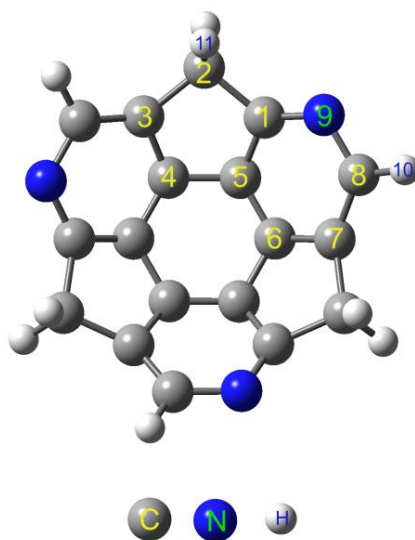
The molecules were optimized by the B3LYP functional with the 6-31G (d,p) basis sets. It can be found from [Scheme S1](#) and [Table S1](#) that doping nitrogen in Sum makes little impact on the C-C bond length and C-H bond length of the Sum skeleton. Obviously, TAS has much shorter C-N bond length and smaller bond angle than the corresponding C-C bond length and C-C-C bond angle of Sum. Moreover, it shows that the N-doping in Sum not only decreases the dipole moment, but also changes its direction, compared with the values of Sum, which also has been reported previously. As for the frontier orbitals shown in [Figure S1](#), the N-doping could dramatically reduce the frontier orbital levels of the Sum, which is consistent with the experiment results, but could not change the degeneracy of the molecular frontier orbitals due to the maintenance of C₃ symmetry. Furthermore, [Figure S2](#) shows that there is little difference of the electronic density contours in LUMO and LUMO+1 between TAS and Sum, but their HOMO and HOMO-1 have significant difference in the bonding or anti-bonding characters of the π electronics on the central phenyl ring of the Sum core. As for the electronic charge density distribution (electrostatic potential, ESP), [Figure S3](#) shows that N-doping in Sum changes the electronic potential of the central phenyl ring from negative to neutral, and the negative electronic potential of TAS almost locates on the nitrogen atoms. This implies that the electrostatic interactions of the TAS dimers should be different from that of Sum dimers. Considering the two enantiomers of (C)-TAS and (A)-TAS that exist in the racemic crystal, the bowl-to-bowl inversion barrier is an essential factor to evaluate the possibility of their isomerization. [Figure S4](#) plots that the inversion barrier of TAS enantiomers reaches 37.78kcal/mol, which is much larger than that of the Sum derivatives (<22kcal/mol) reported in our previous work.^[1] This indicates that N-doping can increase the bowl-to-bowl inversion barrier more dramatically than the substituents in peripheral Sum, implying their better stability of molecular structure in the formation of racemic or homochiral crystals. In a word, when

Supporting Information

doped in Sum, nitrogen atoms could largely change the electronic structure, such as reduce the dipole moment and frontier orbital level, because they play an important role in the electronic effect of the whole buckybowl, though it doesn't change the geometric structures dramatically.

Comparison of the geometries and electronic structures of TAS

Here, we also compared the structures of the optimized molecule under vacuum (TAS-v) with the molecular structure in the solid state, that is in the racemic crystal and in the homochiral crystal by X-ray crystal analysis respectively labeled as TAS-s(*r*) and TAS-s(*c*). From the [Scheme S1](#) and [Table S1](#), it also can be found that the TAS-v has a little larger C-C bond, C-C-C bond angle and a little smaller C-N bond length than those in the solid state. The relative deviation values show that all the geometries of bond length and bond angle between the TAS-v and TAS-s are very closed (<1%), especially their C-H bond length values are all the same. However, the bowl depth of TAS-v is much larger than that of TAS-s(*r*) and TAS-s(*c*). Besides, the dipole moment of TAS-v is similar to that of TAS-s(*r*), but is much larger than that of TAS-s(*c*). As a result, the total energy of TAS-v is closed to that of TAS-s(*r*), but is much lower than that of TAS-s(*c*). [Figure S1](#) also shows the frontier orbital levels of TAS with different structures. Obviously, the TAS-s(*r*) and TAS-s(*c*) both have slightly lower HOMO level, higher LUMO level and larger energy gap than those of TAS-v. Furthermore, the same as TAS-v, TAS-s(*r*) also has twofold degenerate orbitals, while TAS-s(*c*) doesn't have ones.



Scheme S1 The structure of TAS

Supporting Information

Table S1 Selected geometric and electronic structure of TAS molecules optimized under vacuum (TAS-v) and those in the solid state (in racemic and homochiral crystals) by X-ray crystal analysis, respectively labeled as TAS-s(*r*) and TAS-s(*c*), as well as Sum optimized under vacuum. Bond length and bowl depth in angstrom (Å), bond angle in degree (°), dipole moment in Debye, ΔE is the molecular total energy difference in kcal/mol.

	Sum	TAS-v	TAS-s(<i>r</i>)	TAS-s(<i>c</i>)	$\Delta v-s(r)$	$\Delta v-s(c)$	$\Delta/s(r)\%$	$\Delta/s(c)\%$
C1-C2	1.555	1.554	1.553	1.558	0.001	-0.004	0.06	-0.26
C2-C3	1.555	1.551	1.548	1.549	0.003	0.002	0.19	0.13
C3-C4	1.399	1.403	1.393	1.390	0.010	0.013	0.72	0.94
C4-C5	1.433	1.434	1.432	1.436	0.002	-0.002	0.14	-0.14
C1-C5	1.399	1.400	1.394	1.404	0.006	-0.004	0.43	-0.28
C5-C6	1.387	1.387	1.380	1.366	0.007	0.021	0.51	1.54
C6-C7	1.399	1.403	1.393	1.391	0.010	0.012	0.72	0.86
C7-C8	1.400	1.401	1.397	1.399	0.004	0.002	0.29	0.14
C1-N9	1.095	1.331	1.341	1.335	-0.010	-0.004	-0.75	-0.30
C8-N9	1.400	1.371	1.382	1.376	-0.011	-0.005	-0.80	-0.36
C8-H10	1.431	1.088	1.088	1.088	0.000	0.000	0.00	0.00
C2-H11	1.087	1.093	1.094	1.094	-0.001	-0.001	-0.09	-0.09
C1-C2-C3	102.7	101.8	101.6	101.5	0.2	0.6	0.20	0.59
C1-N9-C8	121.2	118.1	117.6	117.7	0.5	0.4	0.43	0.34
Bowl Depth	1.123	1.301	1.260	1.264	0.041	0.037	3.25	2.93
Dipole Moment	1.94(+)	0.47(-)	0.50(-)	0.38(-)	-0.03	0.09	-6.00	23.68
ΔE		0	0.73	2.68				

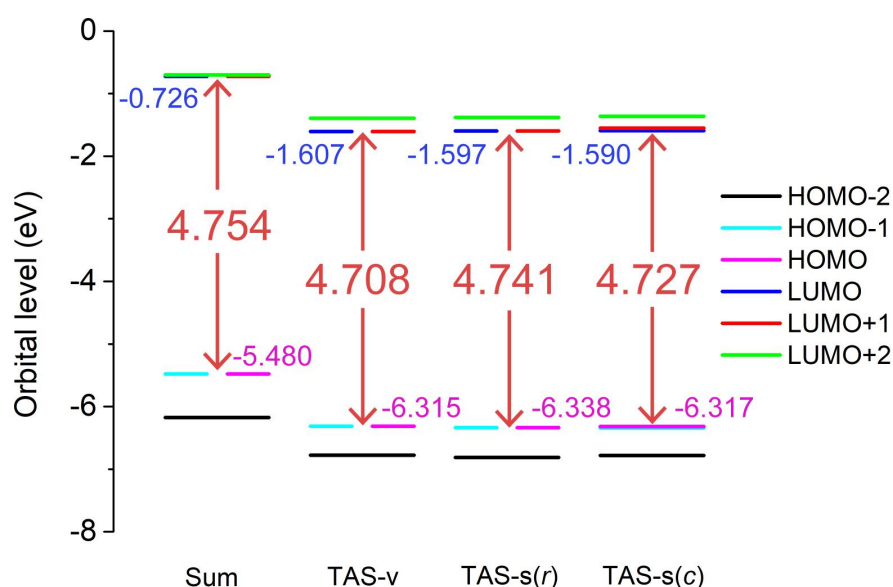


Figure S1 The frontier orbitals level of the Sum and TAS with different monomers.

Supporting Information

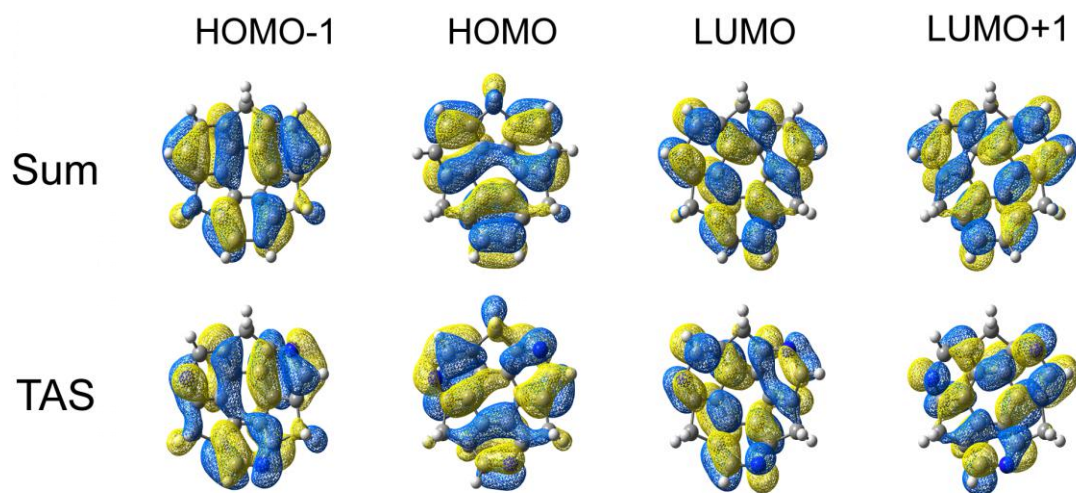


Figure S2 Electronic density contours of the frontier orbital of Sum and TAS both optimized under vacuum.

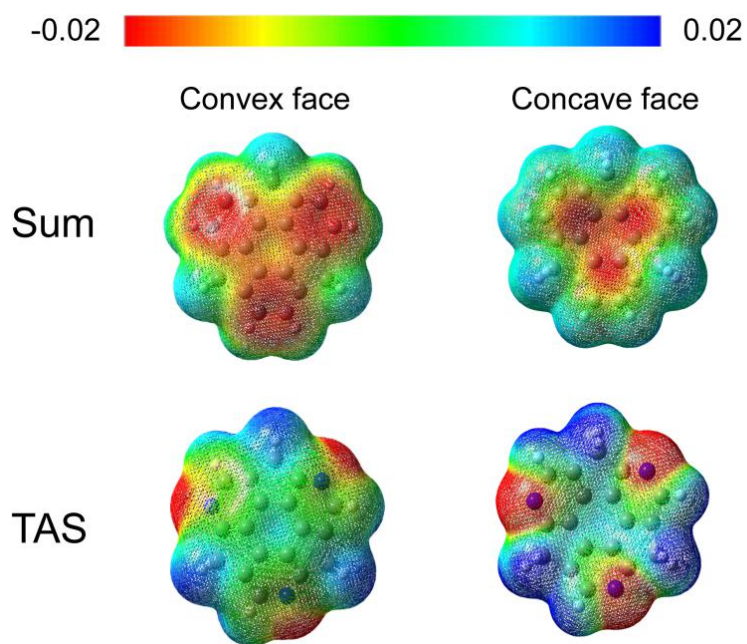


Figure S3 Calculated electrostatic potential (ESP) onto an electron density isosurface of 0.001 a.u. for Sum and TAS both optimized under vacuum.

Supporting Information

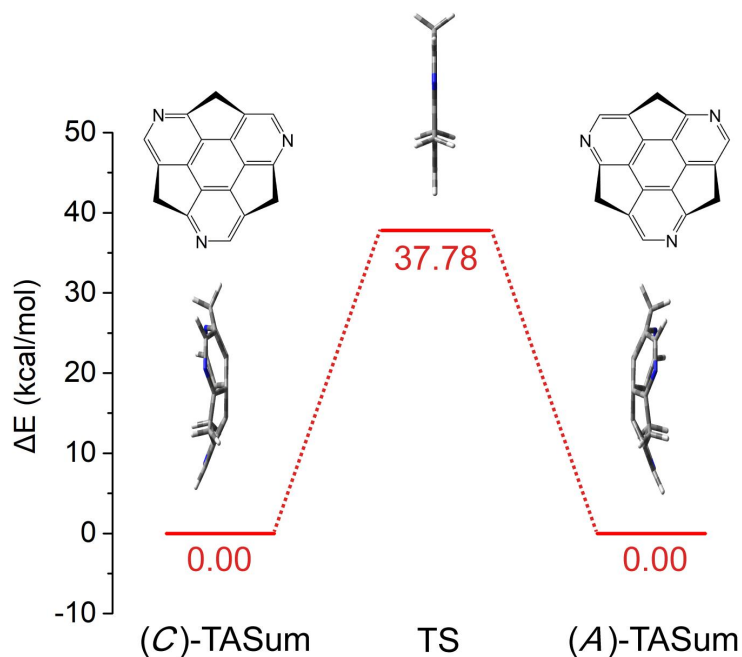


Figure S4 The inversion barrier of the TAS calculated under vacuum.

The optimal conformation of the dimer built by the monomers selected in crystals

The molecular dimer with frozen monomers those selected in the racemic crystal in experiment (TAS- $s(r)$) were built as racemic (TAS- $s(r)-r$) and homochiral (TAS- $s(r)-c$) molecular dimer respectively as well. Figure S5 shows their interaction energy surface. Because the interaction energies of the dimers at their optimal vertical separation fluctuate with the rotation angle, the interaction energy curves of the dimers are drawn in Figure S6, including that of the TAS- $s(c)-c$ dimer (the monomer selected in the homochiral crystal in experiment was built as the homochiral molecular dimer) in comparison. It shows the shape of the curves is almost the same. Nevertheless, the optimal vertical separation of TAS- v ($Z \approx 3.9 \text{ \AA}$) is larger than that of TAS- $s(r)-r$ ($Z \approx 3.8 \text{ \AA}$), consisted with the experiment which is tested as 3.82 \AA , mainly because TAS- v has larger bowl depth (1.301 \AA) than TAS- $s(r)$ (1.260 \AA).

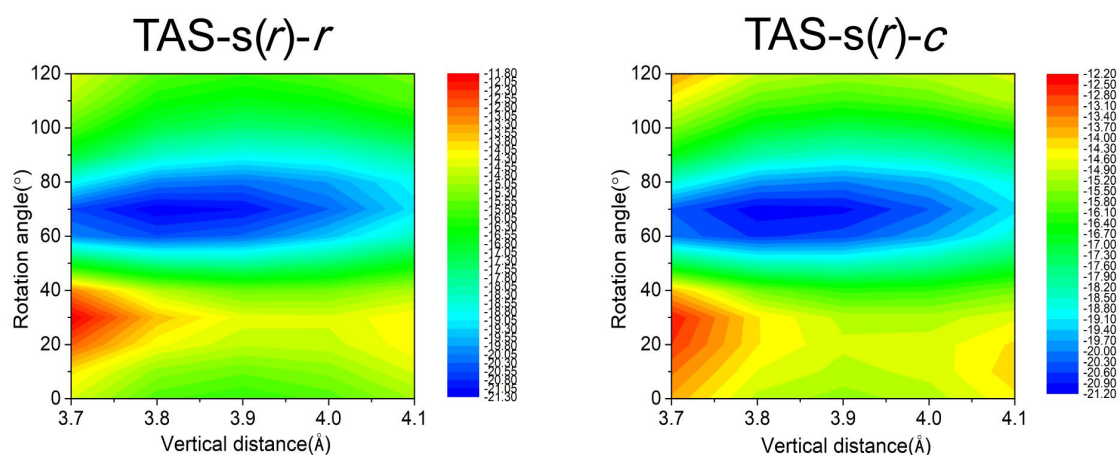


Figure S5 Interaction energy surface (IES) of molecular dimer with frozen monomers that selected in the racemic crystal by X-ray analysis (TAS- $s(r)$). The dimer model is

Supporting Information

built by perpendicular columnar stacking respectively with racemic (TAS-*s(r)-r*) conformation and homochiral (TAS-*s(r)-c*) conformation. The values are given in kcal/mol and the negative sign means the attractive interactions.

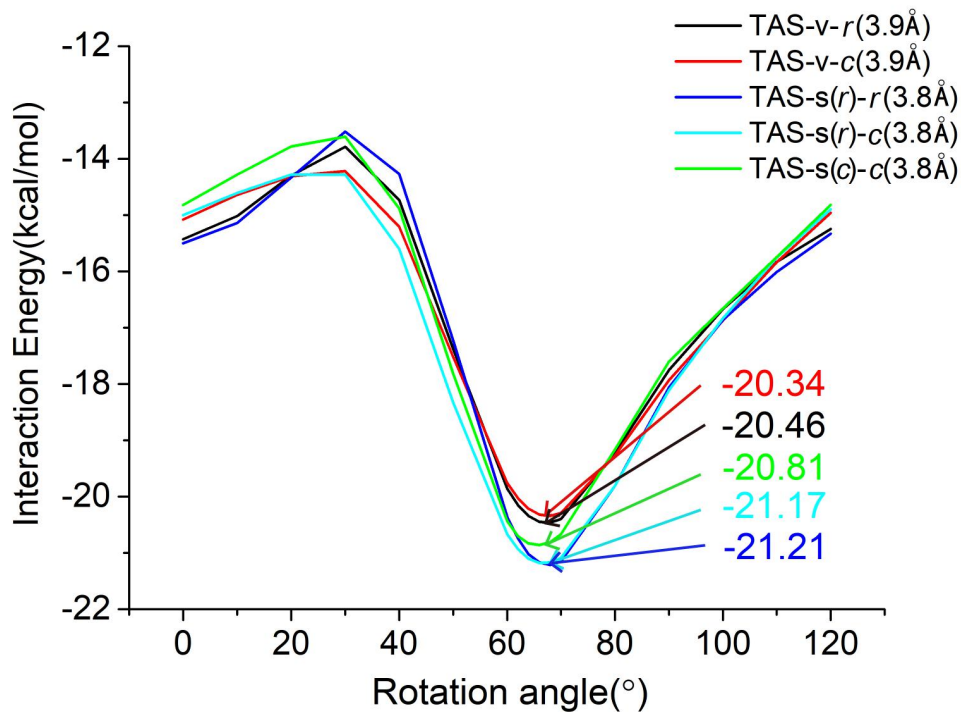


Figure S6 The interaction energy curves of the dimers varying with rotation angle at their respective optimal vertical separation.

Supporting Information

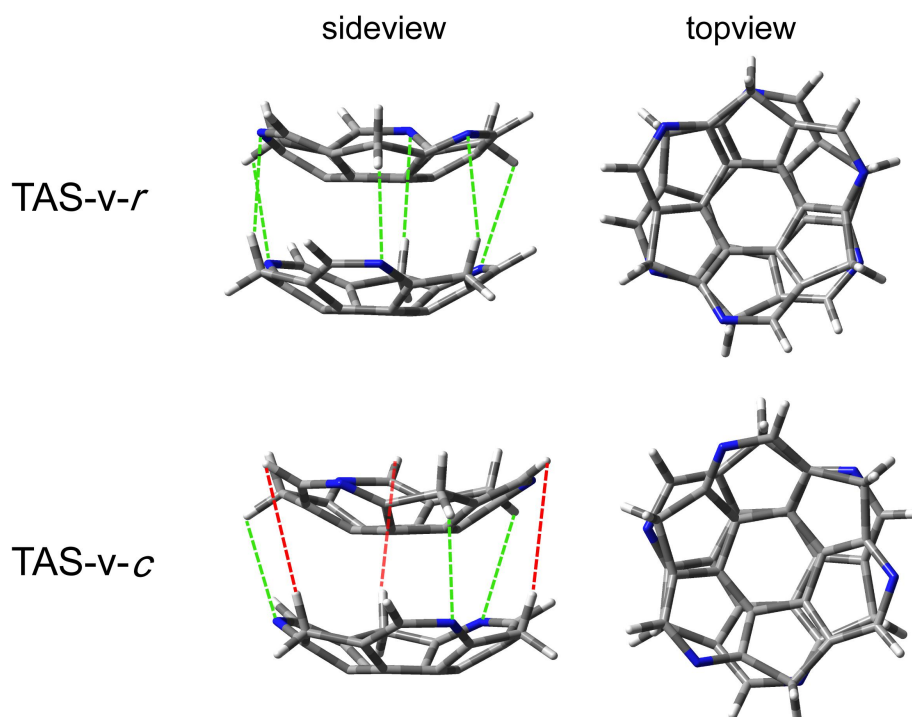


Figure S7 The side view and top view of the optimal conformation ($Z=3.9\text{\AA}$, $\theta=68^\circ$) of the TAS racemic dimer (TAS-v-r) and the homochiral dimer (TAS-v-c) based on the interaction curve by calculation (Green/red line means attractive/repulsive interactions).

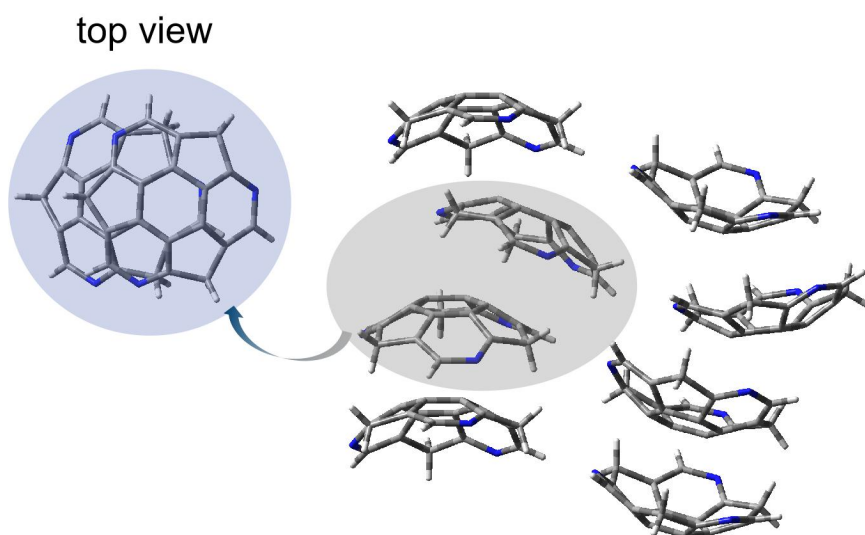


Figure S8 The top view of the molecular packing along the slide column in the TAS homochiral crystal.

Supporting Information

Calculation of transfer integral values

Table S2 Transfer integral values (in eV) calculated by different molecular orbitals, as well as the effective transfer integrals (t_h or t_e) by the combinations of their values (Square root of sum of squares).

TAS- <i>v-r</i> dimer										
Rotation angle	H-1/H-1	H/H-1	H-1/H	H/H	t_h	L/L	L/L+1	L+1/L	L+1/L+1	t_e
0	0.00573	0.05927	0.05699	0.01071	0.08312	0.05757	0.12672	0.12522	0.05476	0.19507
10	0.01210	0.04608	0.04578	0.01690	0.06819	0.03165	0.14617	0.14496	0.02776	0.21012
20	0.02679	0.01928	0.01997	0.02426	0.04557	0.15063	0.01691	0.01522	0.15203	0.21522
30	0.04258	0.01665	0.01575	0.04391	0.06532	0.08738	0.11764	0.11862	0.09059	0.20917
40	0.02590	0.07575	0.07013	0.02622	0.10961	0.14181	0.00303	0.00186	0.14952	0.20611
50	0.04361	0.08849	0.08275	0.04840	0.13756	0.09554	0.10204	0.10887	0.10795	0.20748
60	0.01017	0.10509	0.09626	0.00960	0.14320	0.08106	0.10628	0.12381	0.08059	0.19922
70	0.08821	0.01731	0.02214	0.09804	0.13485	0.09140	0.06954	0.08653	0.09919	0.17469
80	0.00287	0.07291	0.07043	0.01287	0.10222	0.10235	0.01612	0.03352	0.10049	0.14818
90	0.02671	0.01836	0.01694	0.02224	0.04280	0.07397	0.06616	0.06152	0.08672	0.14544
100	0.01204	0.01329	0.01625	0.00547	0.02481	0.11255	0.00787	0.01464	0.11586	0.16238
110	0.05139	0.00289	0.01547	0.04727	0.07158	0.12386	0.03134	0.03341	0.11998	0.17843
120	0.04830	0.04558	0.03290	0.04115	0.08477	0.13745	0.02901	0.03006	0.12996	0.19372
TAS- <i>v-c</i> dimer										
Rotation angle	H-1/H-1	H/H-1	H-1/H	H/H	t_h	L/L	L/L+1	L+1/L	L+1/L+1	t_e
0	0.04515	0.01208	0.01180	0.04476	0.06578	0.13091	0.00710	0.00678	0.13265	0.18663
10	0.01270	0.03122	0.03076	0.01331	0.04753	0.11736	0.08720	0.08578	0.11687	0.20590
20	0.00678	0.00151	0.00159	0.00593	0.00927	0.10503	0.10899	0.10987	0.10354	0.21378
30	0.01342	0.04514	0.04501	0.01411	0.06665	0.01880	0.14365	0.14155	0.02095	0.20363
40	0.02731	0.08353	0.08182	0.02977	0.12371	0.01674	0.13495	0.13181	0.01377	0.18988
50	0.03417	0.10402	0.10168	0.03042	0.15249	0.09636	0.09652	0.09607	0.09026	0.18968
60	0.00691	0.10961	0.10891	0.00277	0.15470	0.03618	0.13704	0.13219	0.02882	0.19594
70	0.05762	0.08398	0.08305	0.05353	0.14190	0.11509	0.05808	0.06630	0.12240	0.18973
80	0.07910	0.00949	0.00963	0.07496	0.10981	0.11799	0.01729	0.00634	0.11809	0.16795
90	0.03913	0.01739	0.01522	0.03853	0.05958	0.10831	0.00059	0.00767	0.10551	0.15140
100	0.02152	0.00103	0.00471	0.01928	0.02929	0.06329	0.08934	0.08783	0.06549	0.15489
110	0.01935	0.03105	0.03793	0.01645	0.05521	0.03970	0.11056	0.11215	0.04320	0.16806
120	0.03070	0.03318	0.02970	0.03862	0.06646	0.13161	0.00601	0.01144	0.13072	0.18595
TAS- <i>s(r)-r</i> dimer										
Rotation angle	H-1/H-1	H/H-1	H-1/H	H/H	t_h	L/L	L/L+1	L+1/L	L+1/L+1	t_e
0	0.02198	0.06235	0.06624	0.02474	0.09680	0.11400	0.05172	0.05962	0.10967	0.17678
10	0.04386	0.03683	0.04195	0.04348	0.08325	0.04372	0.13255	0.12860	0.05135	0.19661

Supporting Information

20	0.04095	0.01257	0.01198	0.03700	0.05786	0.06727	0.13768	0.12995	0.06453	0.21103
30	0.00075	0.04857	0.04877	0.00398	0.06895	0.14007	0.06340	0.06250	0.13244	0.21234
40	0.02392	0.07630	0.07628	0.02985	0.11447	0.12487	0.08200	0.08735	0.12367	0.21270
50	0.09733	0.03918	0.02936	0.09740	0.14614	0.15081	0.00969	0.00569	0.15219	0.21455
60	0.05079	0.10103	0.08985	0.05488	0.15450	0.03094	0.14361	0.13691	0.03230	0.20339
70	0.07293	0.07757	0.06666	0.07730	0.14750	0.07887	0.09959	0.09542	0.07161	0.17427
80	0.07645	0.02172	0.01676	0.08344	0.11644	0.08069	0.06720	0.06088	0.07716	0.14383
90	0.00315	0.03926	0.03711	0.00182	0.05415	0.09538	0.01592	0.02171	0.09868	0.13986
100	0.01508	0.00909	0.00386	0.01540	0.02371	0.04569	0.09488	0.10276	0.04908	0.15511
110	0.03175	0.03882	0.04504	0.04104	0.07892	0.08325	0.07668	0.08626	0.08451	0.16550
120	0.06253	0.04178	0.03261	0.05306	0.09764	0.12182	0.01382	0.00600	0.12755	0.17702

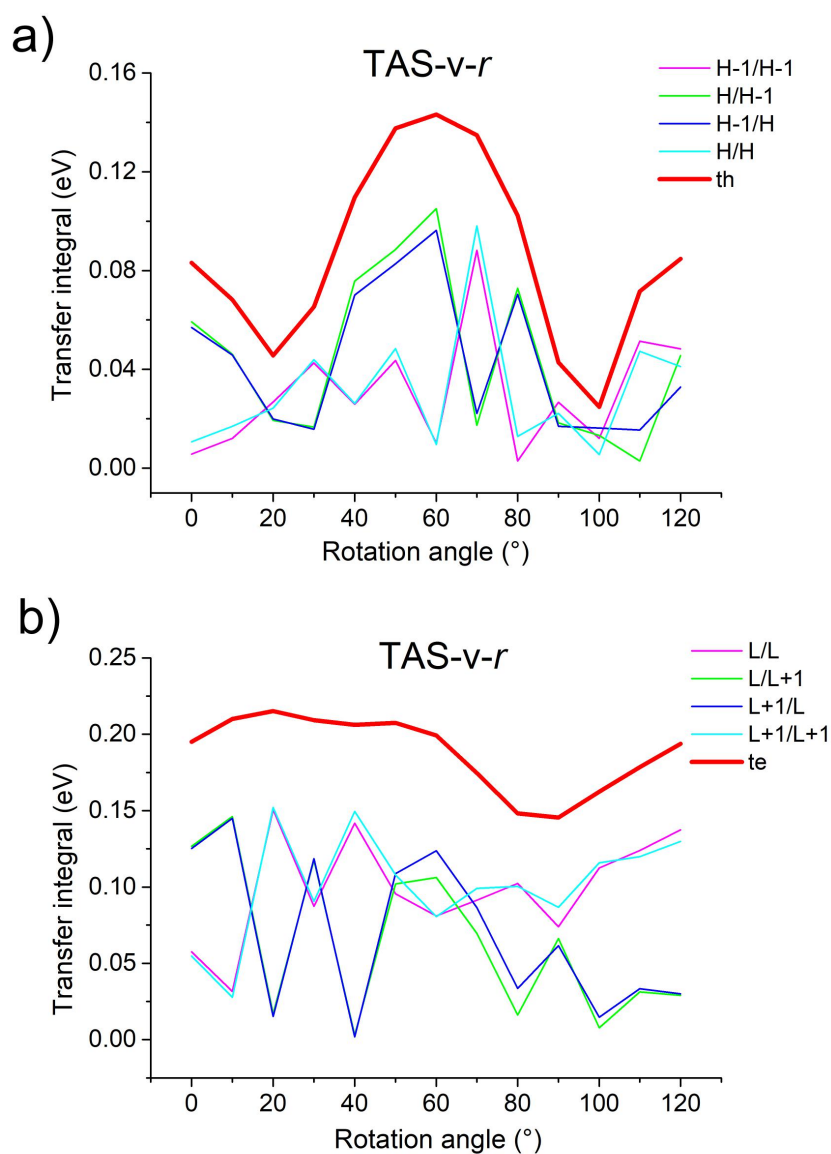


Figure S9 Variation of the a) hole and b) electron effective transfer integrals (*th* and *te*), as well as the corresponding transfer integrals involving different molecular orbitals for TAS-*v-r* dimer at its optimal vertical separation (3.9Å) with the rotation

Supporting Information

angle in dimer model.

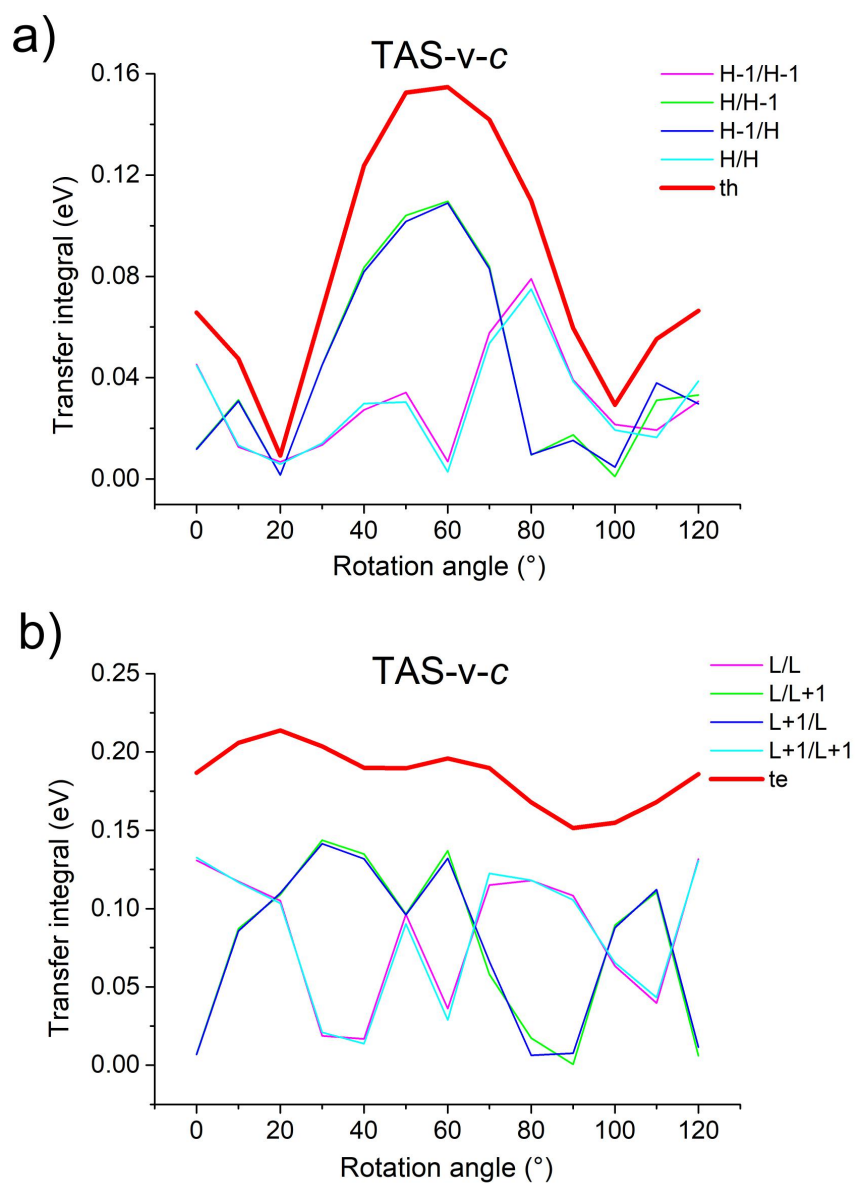


Figure S10 Variation of the a) hole and b) electron effective transfer integrals (t_h and t_e), as well as the corresponding transfer integrals involving different molecular orbitals for TAS-v-c dimer at its optimal vertical separation (3.9 Å) with the rotation angle in dimer model.

Supporting Information

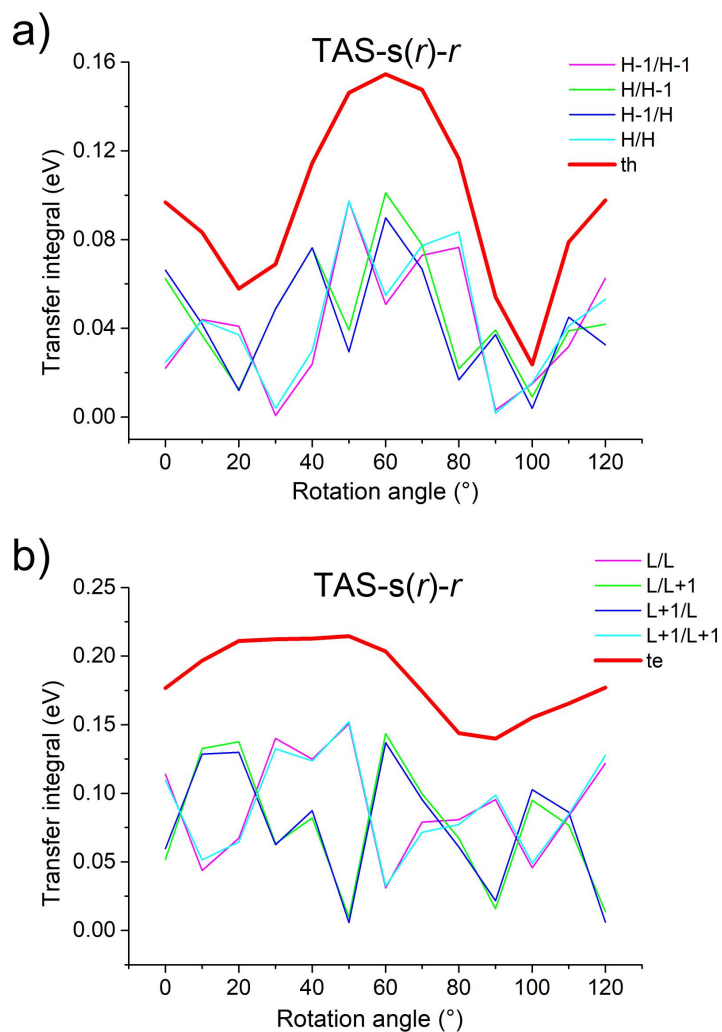


Figure S11 Variation of the a) hole and b) electron effective transfer integrals (*th* and *te*), as well as the corresponding transfer integrals involving different molecular orbitals for TAS-s(*r*)-*r* dimer at its optimal vertical separation (3.8Å) with the rotation angle in dimer model.

Supporting Information

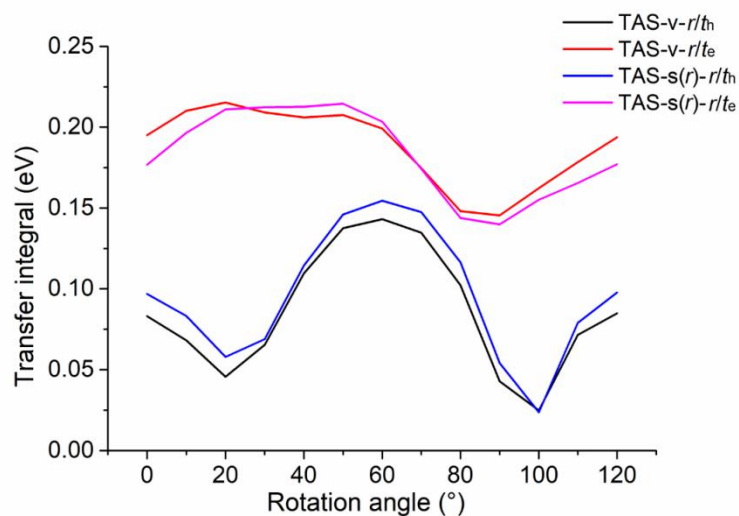


Figure S12 The variation of effective transfer integrals (t_h or t_e) for TAS-v-r dimer and TAS-s(r)-r dimer at their respective optimal vertical separation (3.9 Å and 3.8 Å) with the rotation angle in dimer model.

As the simplest approach, the Energy-Splitting-in-Dimer (ESD) Method has been widely used for the estimation of transfer integrals in organic semiconductors. Here, the Koopmans' theorem (KT) is applied based on the one-electron approximation to make a comparison with the Direct coupling (DC) method to describe the variation of the charge transfer integrals with the rotation angle of the molecular dimers.^[2]

$$t_h = \frac{E_H - E_{H-1}}{2}$$

$$t_e = \frac{E_{L+1} - E_L}{2}$$

t_h or t_e is hole or electron transfer integral respectively, E_H/E_{H-1} is the energy of HOMO/HOMO-1, and E_{L+1}/E_L is the energy of LUMO+1/LUMO, which are obtained from the neutral state of two stacked molecules with the closed shell configuration.

Supporting Information

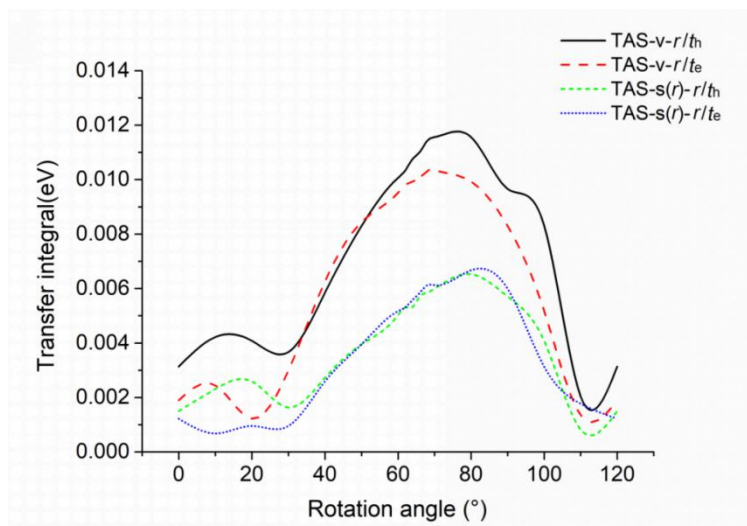


Figure S13 Variation of the charge transfer integral of the racemic dimer built by TAS monomer optimized under vacuum (TAS-v-r) and selected in the racemic crystal (TAS-s(r)-r) respectively at their optimal vertical separation (3.9Å and 3.8Å) with the rotation angle (°) by KT method.

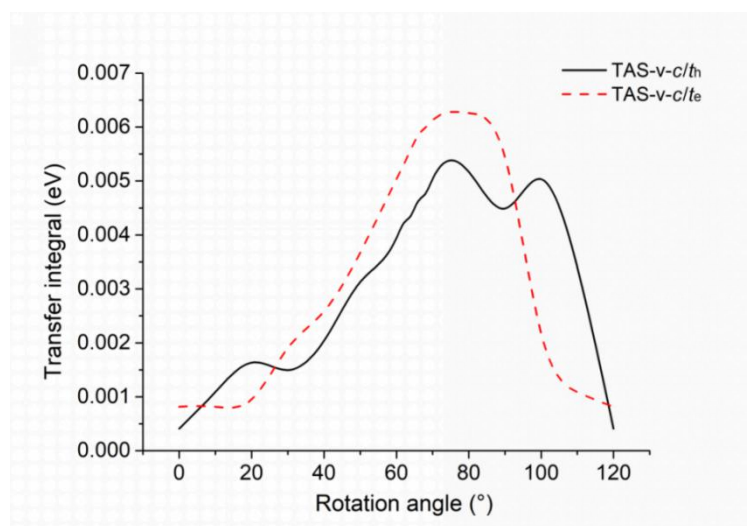


Figure S14 Variation curves of the charge transfer integral of the homochiral dimer calculated by eclipsed columnar stacking dimer model using TAS monomer optimized under vacuum (TAS-v-c) at the optimal vertical separation (3.9Å) as a function of the rotation angle (°) by KT method.

References

- [1] X. Chen, F.Q. Bai, Y. Tang, H.X. Zhang, How the substituents in corannulene and sumanene derivatives alter their molecular assemblings and charge transport properties?--A theoretical study with a dimer model, *J Comput Chem*, 37 (2016) 813-824.
- [2] X.K. Chen, L.Y. Zou, A.M. Ren, J.X. Fan, How dual bridging atoms tune structural and optoelectronic properties of ladder-type heterotetracenes?--a theoretical study, *Phys Chem Chem Phys*, 13 (2011) 19490-19498.